Pattern formation of coupled spiral waves in bilayer systems: Rich dynamics and high-frequency dominance

Haichun Nie,[1,2] Jihua Gao,[3] and Meng Zhan[1,*]

[1]*Wuhan Institute of Physics and Mathematics, Chinese Academy of Sciences, Wuhan 430071, China*

[2]*Graduate School of the Chinese Academy of Sciences, Beijing 100049, China*

[3]*Shenzhen Key Laboratory of Special Functional Materials, College of Materials, Shenzhen University, Shenzhen 518060, China*

(Received 1 June 2011; revised manuscript received 7 September 2011; published 7 November 2011)

The interaction of two spiral waves with independent frequencies in a bilayer oscillatory medium (one spiral in each layer) and with a symmetric coupling e is studied. If the spirals have *different* frequencies, the faster spiral is unaffected by the slower one, and the slower can show a variety of behaviors, which depend on e and include, in order of increasing e, phase drifting, amplitude modulation, amplitude domination, and phase synchronization. This high-frequency dominance, the asymmetric driving-response effect under the condition of a symmetric coupling, is generic and independent of whether the coupled spiral waves are outwardly rotating or inwardly rotating spirals. If the spirals have *identical* frequencies, they may even show complete synchronization, parallel drift, or circular drift, depending on the relative rotation direction of the two spirals and their initial separation distance. Comparisons with coupled spirals in monolayer media, previous works on coupled spirals in bilayer systems, and coupled phase oscillators are made.

DOI: 10.1103/PhysRevE.84.056204 PACS number(s): 89.75.Kd, 82.40.Ck, 05.45.Gg, 47.27.Rc

I. INTRODUCTION

Spiral waves in both excitable and oscillatory media have been widely observed in diverse systems [1–5]. The interaction of several spiral waves in one spatial domain is one of the central problems in the study of spiral wave dynamics [6–17]. It has been well accepted that a universal frequency-dependent dominance exists in the interaction [14–16], namely, the high-frequency spiral can invade and suppress the domain of the low-frequency spiral, and finally drive it out of the observable region. This behavior is for the usual outward-rotating spiral. Therefore, more specifically, it is high-frequency dominance. For two inward-rotating spiral waves (i.e., antispirals), the invading direction is just opposite, and the behavior becomes low-frequency dominance [14,17]. More complicated patterns are possible in some other situations, such as in strongly inhomogeneous media.

The interaction of spiral waves in multilayer systems is also of great significance, since most of our real systems are three dimensional (e.g., chemical reaction-diffusion systems and cardiac tissue); they can be treated as linearly coupled layers if they are sufficiently thin but meanwhile the third dimension cannot be completely ignored. Clearly the bilayer system represents an intermediate state between monolayer and three-dimensional systems.

The experimental study of the interaction of spiral waves in two coupled layers was pioneered by Winston *et al*. [18]. They investigated chemical waves propagating on the surface of a ferroin-loaded Nafion membrane suspended in a continuous-flow stirred-tank reactor pumped with a Belousov-Zhabotinsky reaction mixture, and found that the coupling can always lead to complete spatiotemporal entrainment of two spirals, showing an amplitude-modulated pattern in the transient. The phenomenon of the high-frequency spiral dominating over the low-frequency spiral throughout the evolution was there reported for the first time, when two spiral waves with slightly different rotation periods were coupled. Since then, it has aroused great interest continuously [19–27]. The same group studied two domains of excitable media with distributed *identical* Belousov-Zhabotinsky systems that are locally coupled to each other by means of a video camera–video projector setup [19], and discovered that different rotations (i.e., chiralities) or initial separation distances of the two spirals may also essentially determine the final spiral patterns. [Note that the chirality, which denotes the handedness in the spatial structure of spiral waves, is fundamentally different from the usual spiral (or antispiral) for outward-rotating spiral (or inward-rotating spiral) property, which indicates the direction of propagation in time.] In a model study of two spiral waves in linearly coupled reaction-diffusion systems, the high-frequency dominance effect was supported by detailed numerical simulations, and two fundamental types of spiral pattern including phase-drifting and phase-synchronized spirals was documented [23]. Recently we studied the interaction of spirals in a bilayer system with negative-feedback couplings, which can be different, and found that under the condition of strongly asymmetric coupling, an amplitude-dominated spiral exists, featuring the appearance of a spiral pattern in the amplitude and absence of a singularity tip point [26]. A model of three coupled layers has also been studied recently [28]. Based on these separate findings, a unified physical picture remains obscure and some interesting questions naturally arise: What is the relation between all these reported patterns, such as phase-synchronized [18,23,26], amplitude-modulated [18], phase-drifting [23], and amplitude-dominated [26] patterns? Is the high-frequency dominance generic? Will it change if two outwardly rotating spirals are replaced by two inwardly rotating spirals? What will happen for two identical spirals in bilayer oscillatory media? What is the effect of different chiralities?

In this work, with the above-mentioned motivations we will study the interaction of two spiral waves in a bilayer system described by a model of two linearly coupled complex

*zhanmeng@wipm.ac.cn

Ginzburg-Landau equations (CGLEs), and we are concerned with possible generic behaviors in such an interaction. This choice is based on two facts: (1) the CGLE is the normal form of a spatiotemporal system at the onset of a Hopf bifurcation, and it has become a standard model for pattern research in oscillatory media [4,5], and (2) we can easily obtain the usual outward- or inward-rotating spiral (antispiral) for different system parameters in the CGLE model, while it is generally believed that antispirals cannot be observed in excitable media. We find that the coupled dynamical behaviors are indeed very rich, and the high-frequency dominance does reappear but in a different manner.

II. MODEL

We consider the following model of linearly coupled CGLEs [29–35]:

$$\partial_t A_{1,2} = \mu_{1,2} A_{1,2} - (1 + i\alpha)|A_{1,2}|^2 A_{1,2} + (1 + i\beta)\nabla^2 A_{1,2} + e(A_{2,1} - A_{1,2}), \quad (1)$$

where the systems 1 and 2 are denoted by the subscripts 1 and 2, respectively, and $\nabla^2 = \frac{\partial^2}{\partial x^2} + \frac{\partial^2}{\partial y^2}$. $A_{1,2}$ are complex variables [$A = \mathrm{Re}(A) + \mathrm{Im}(A)i$], α and β are the system parameters, $\mu_{1,2}$ are scale parameters, and e represents the negative-feedback coupling strength between the two layers. In the numerical simulations, we used the forward Euler method for the time integration with the time step $\Delta t = 0.005$, and a five-point spatial difference method for the Laplacian for each layer, having 256×256 space units with the space step $\Delta x = \Delta y = 0.5$. Nonflux boundary conditions were used throughout this work. The different scale parameters μ_1 and μ_2 were chosen for the two coupled layers to represent the system's linear inhomogeneity. The benefit of this setting is that the initial rotation frequencies (or wavelengths) of two spiral waves can be easily connected by a scale: $\omega_{10} = \mu_1\omega_0$, $\omega_{20} = \mu_2\omega_0$, and $\omega_{10} = \frac{\mu_1}{\mu_2}\omega_{20}$, where ω_0, ω_{10}, and ω_{20} denote the spiral wave frequencies for $\mu_0 = 1$, μ_1, and μ_2, respectively [4,5,14]. Without losing generality, we always choose a fixed μ_2 ($\mu_2 = 3.0$) with the value of μ_1 finely tuned. It should be noted that the CGLE has an extremely rich structure and with it very complicated spatiotemporal dynamical behaviors are possible. Here we study only the coupled dynamics of two spiral waves, which have been well prepared before the coupling.

III. OBSERVATIONS

We start from the interaction of two outwardly rotating spiral waves. As an example, a parameter set $\alpha = -0.4$ and $\beta = -1.5$ is selected [15,36]. Thus $\omega_0 \approx 0.421$ and $\omega_{20} = \mu_2\omega_0 \approx 1.263$. Two spirals with the same chirality and sufficiently far apart are first considered. The phase diagrams in the (e,μ_1) parameter space for systems 1 and 2 are shown in Figs. 1(a) and 1(b), respectively. In the figures, the numbers from 0 to 4 are used to represent five major different types of pattern: minimal modification, phase-drifting, amplitude-modulated, amplitude-dominated, and phase-synchronized patterns, respectively. All reported pattern forms can be found here. The phase-synchronization region (type 4) has been well

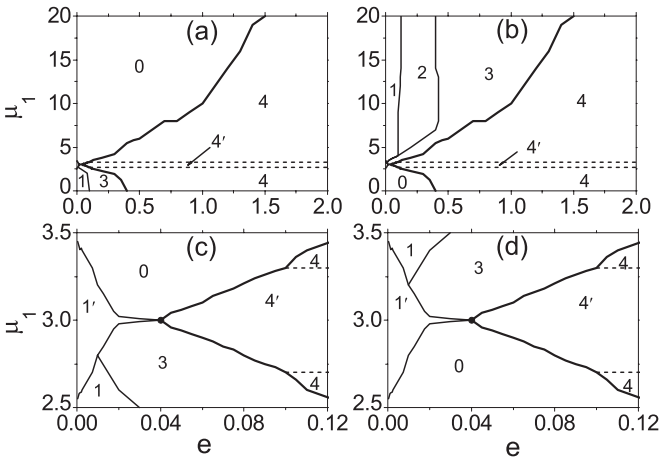

FIG. 1. (a), (b) Phase diagrams of systems 1 and 2, respectively, in the interaction of a pair of spirals in a bilayer oscillatory medium (1). The number 0 represents that the faster spiral is only slightly modified, the numbers 1, 2, and 3 represent phase-drifting, amplitude-modulated, and amplitude-dominated patterns of the slower spiral, and the number 4 indicates phase synchronization between two spiral waves. (c), (d) Detailed phase diagrams of systems 1 and 2 around $\mu_1 = \mu_2 = 3.0$, showing two additional subtypes of patterns: type 1′ for the double-phase-drifting pattern and type 4′ for the phase-synchronized-and-multispiral pattern. The critical point at $\mu_1 = \mu_2 = 3.0$ and $e_c \approx 0.04$ has been emphasized by a black point. $\alpha = -0.4$ and $\beta = -1.5$ within the outward-rotating spiral parameter region.

separated from all other regions, and the parameter boundaries have been emphasized by several heavy solid lines. The tongue structure is clear, and it gets wider with the increase of e, reminiscent of the Arnold tongue, which has been broadly observed in coupled (or forced) oscillators with frequency mismatch. Out of the whole phase-synchronization region for smaller e, surprisingly we find that the fast spiral pattern is only slightly modified, denoted by the number 0, and in contrast the slow spiral has to be enslaved for different system parameters, which are denoted by either type 1, 2, or 3. This is correct for the parameters $\mu_1 > \mu_2 = 3.0$ and $\mu_1 < \mu_2 = 3.0$, indicating the establishment of an asymmetric driving-response relationship between the two symmetrically coupled spiral waves in the whole parameter space.

Figure 2 shows the detailed patterns for different system parameters. For the first five columns, from left to right, $e =$ 0.0, 0.08, 0.3, 0.5, and 1.5, which correspond to the initial patterns and patterns of types 1, 2, 3, and 4 for system 2, respectively; $\mu_1 = 14.0$. For the rows, from top to bottom, the patterns for $\mathrm{Re}(A_1)$, $\mathrm{Re}(A_2)$, $|A_1|$, and $|A_2|$ are illustrated. In addition, the fast Fourier transform (FFT) spectra for systems 1 and 2 of an arbitrarily chosen spatial point, which is far from the spiral tip and boundaries in the pattern of $\mathrm{Re}(A)$, are given in the last two rows. Clearly the frequency of the highest peak (ω_{1c} or ω_{2c}) is identical to the rotation frequency of the spiral wave, and its height (F_{1c} or F_{2c}) represents the periodicity strength of the spiral wave.

For the two spiral waves in each layer as initial conditions, as shown in the first column ($e = 0.0$), their tips have been chosen to be sufficiently distant. Their different wavelengths

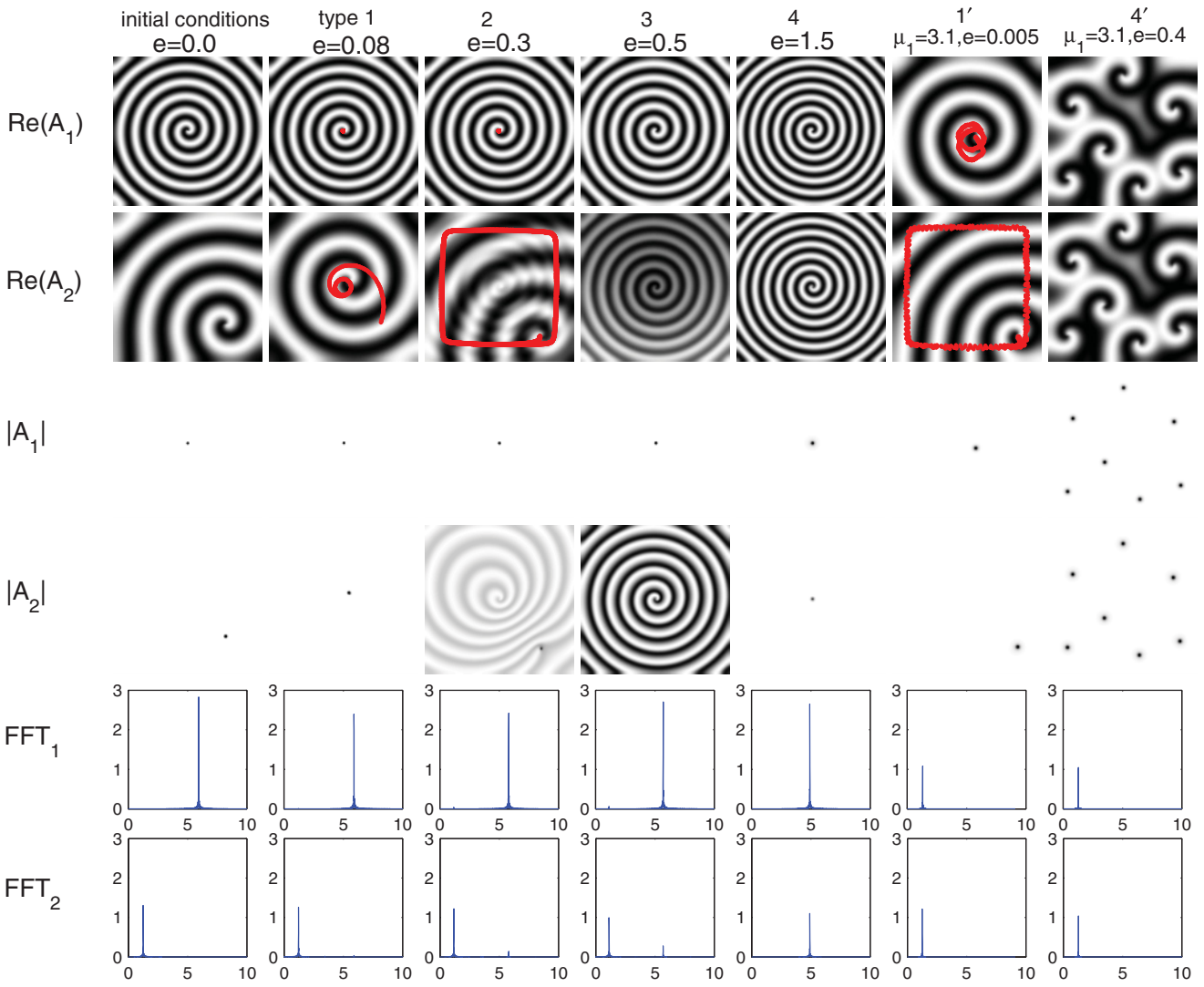

FIG. 2. (Color online) Pattern formation development and frequency spectrum analysis for the interaction of two outwardly rotating spirals with independent rotation frequencies. From left to right, initial conditions and patterns of types 1 (phase drifting), 2 (amplitude modulated), 3 (amplitude dominated), 4 (phase synchronized), 1′ (double phase drifting), and 4′ (phase synchronized and multispiral) are listed. $\alpha = -0.4$ and $\beta = -1.5$. For the first five columns, $\mu_1 = 14.0$.

(frequencies) can be easily recognized by the comparison between Re(A_1) and Re(A_2) (FFT1 and FFT2). As e increases, e.g., $e = 0.08$ in the second column, the slow spiral wave 2 begins drifting, and after a short transient, it becomes slaved by the fast spiral wave 1 and periodically rotates around a very small circle. This phenomenon is obvious in the pattern of Re(A_2) with the tip trajectory superimposed. As e increases further, e.g., $e = 0.3$ in the third column, the slow spiral 2 not only periodically drifts in its phase, but also is slightly modulated by the amplitude of the fast spiral 1. This is clear in the patterns of Re(A_2) and $|A_2|$, where its tip (black point) remains. In the fourth column ($e = 0.5$), an amplitude-dominated pattern on layer 2 appears, where it seems that the amplitude of the slow spiral 2 has been totally imprinted and anchored by that of spiral 1, and meanwhile its own tip is lost as shown in the pattern of $|A_2|$. This type of pattern has been observed in two identical spiral waves in a bilayer system but with an asymmetric coupling [26]. Here we find that the same type of pattern actually can broadly occur in two coupled spiral waves with different independent frequencies and even under a symmetric coupling. In contrast to the amplitude-modulated spiral wave for type 2, clearly this is a stronger amplitude effect. Comparing the first four patterns of Re(A_1) for system 1 in the top row, we are surprised that we cannot find any distinction between them. However, comparing the first four plots of FFT1 in the fifth row, we do find some slight changes in both the peak positions and their heights. Finally, when e is sufficiently large, shown in the fifth column for $e = 1.5$, the two spiral waves become phase synchronized with an identical wavelength and rotation frequency. Their frequency peak heights can still be different. The tip of spiral 2 is recreated, as shown in the center of the pattern of $|A_2|$. These patterns indicate that the faster spiral 1 is dominant in the interaction and the slower spiral 2 is only slaved, and interestingly this dominance appears for all different types of pattern. Thus it is an extension of the dominance of faster

spirals in monolayer media and also of the dominance for only certain types of pattern in previous observations [18,23,26].

So far all different types of pattern formation due to interaction have been well classified and illustrated. A clear picture based on these phenomenological observations can be well established: the faster spiral always plays a dominant role in the interaction and shows a minimal modification, whereas the slower one has to gradually change with a change in coupling strength e—in order of increasing e, it shows phase-drifting (for a pure phase effect), amplitude-modulated (for a weak amplitude effect), amplitude-dominated (for a strong amplitude effect), and phase-synchronized (for a united phase-and-amplitude effect) patterns. In Figs. 1(a) and 1(b), we also find that some types of pattern may not exist due to different system parameters.

To quantitatively characterize the transitions from one type to another, we calculate the frequency peak position ω_c and its height F_c in FFT for both systems. The results for ω_{1c} (open circles) and ω_{2c} (open and filled triangles) and F_{1c} (open circles) and F_{2c} (open and filled triangles) as functions of e are shown in Figs. 3(a) and 3(b), respectively. $\alpha = -0.4$, $\beta = -1.5$, and $\mu_1 = 14.0$, which are the same as the parameters used in the first five columns in Fig. 2. Three vertical dashed lines are added to indicate the threshold couplings for the transitions. In addition, the tip number n vs e is plotted with a solid line to denote the vanishing of the tip ($n = 0$) within the amplitude-dominated spiral region for type 3. Based on these calculations, all four distinct types of behavior in layer 2 can be easily divided. In Fig. 3(a), both ω_{1c} and ω_{2c} slightly change with e, and a jump from two values (two frequency peaks) to a single value (one frequency peak) of ω_{2c} is clear just prior to the phase synchronization (type 4) region. The latter indicates a clear directionality effect from the fast spiral 1 to the slow spiral 2. We also calculate ω_{1c} and ω_{2c} for different μ's and e's; the results are shown in Fig. 3(c). The dashed lines denoted by ω_{10} and ω_{20} are for the initial frequencies of systems 1 and 2 without coupling, respectively, and the middle dashed line is for their average $(\omega_{10} + \omega_{20})/2$. For system 1, from top to bottom, the solid lines are for $e = 0.2$, 0.8, 1.2, 1.6, 10, 20, 40, and 80, whereas for system 2, from left to right, only the first two dotted lines for $e = 0.2$ and 0.8 are discernible. There is a jump from two values to a single value of ω_{2c} before phase synchronization appears again. From this figure, we also know that the final synchronized frequency will saturate to $(\omega_{10} + \omega_{20})/2$ with increase of e.

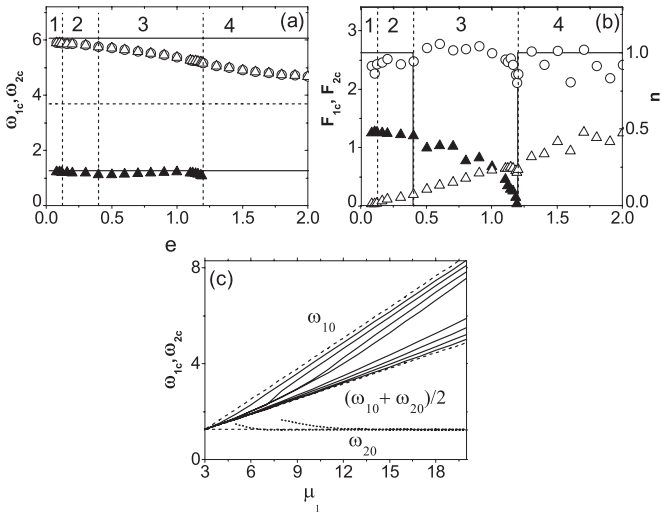

FIG. 3. (a), (b) Plots of the eventual rotation frequencies of spiral waves ω_{1c} (open circles) and ω_{2c} (open and filled triangles), and the peak heights in FFT F_{1c} (open circles) and F_{2c} (open and filled triangles) vs e. $\mu_1 = 14.0$ and $\mu_2 = 3.0$. In (a), a big jump from two values to a single value of ω_{2c} prior to the phase synchronization (type 4) is clear. In (b), the spiral tip number n for system 2 is added with a solid line. (c) ω_{1c} (solid line) and ω_{2c} (dotted line) vs μ_1 for different e's. For system 1, from top to bottom, $e = 0.2$, 0.8, 1.2, 1.6, 10, 20, 40, and 80; for system 2, from left to right, only the first two ω_{2c}'s for $e = 0.2$ and 0.8 are discernible.

In the interaction of two spiral waves in monolayer systems, it has been found that a slight frequency mismatch will produce an immediate invasion from the fast (slow) spiral to the slow (fast) one, if they are outwardly (inwardly) rotating, and coexistence occurs only under the condition that their frequencies are equal to each other or the difference is extremely large [14–17]. Hence there the frequency-dependent dominance is absolute. For the current situation, we find the behaviors can be more varied. In Figs. 1(c) and 1(d), we give more detailed phase diagrams around $\mu_1 \approx \mu_2 = 3.0$ for systems 1 and 2, respectively. Two additional subtypes of pattern (types $1'$ and $4'$) are found. Type $1'$ denotes the double-phase-drifting pattern and type $4'$ denotes the phase-synchronized-and-multispiral pattern. Their patterns and frequency spectra are listed in the last two columns of Fig. 2 for $\mu_1 = 3.1$ and $e = 0.005$ and $\mu_1 = 3.1$ and $e = 0.4$, as two examples. Basically types $1'$ and $4'$ are special cases for $\mu_1 \approx \mu_2$ only, and type $1'$ ($4'$) belongs to type 1 (4). Since here the frequency discrepancy is so small and the dominant effect of the fast spiral over the slow can only be weak, it is easy to understand the occurrence of these two subtypes of pattern as a slight deviation from the pure directionality effect. In the sixth column of Fig. 2 for type $1'$ ($\mu_1 = 3.1$, $\mu_2 = 3.0$, and $\mu_1 \gtrsim \mu_2$), we do find a weaker dominant effect: spiral 1 (2) drifts around a small (large) circle.

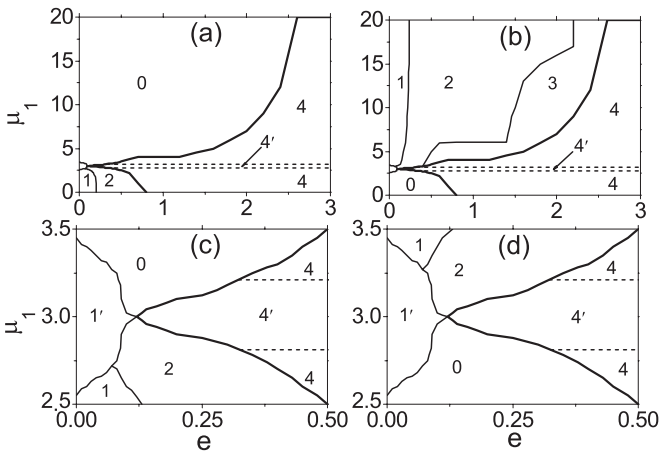

FIG. 4. As Fig. 1, but for two coupled inward-rotating spirals; $\alpha = -1.5$, $\beta = -0.4$, and $\mu_2 = 3.0$. Similar dynamical behaviors have been found and the dominance direction from the fast to the slow spiral is the same.

Since the frequency-dependent dominance in monolayer systems is determined by the medium property: for two coupled antispirals, the invading direction will become opposite and the slow spiral will be dominant in the end [14,17]; here one may naturally ask what will happen in bilayer systems. Extensive simulations and observations demonstrate that here the dominant effect is independent of the properties of the medium, namely, the high-frequency dominance of faster spirals is absolute and no opposite effect exists. As an example, a different parameter set, $\alpha = -1.5$ and $\beta = -0.4$, within the inward-rotating spiral parameter region [36] is chosen and the corresponding phase diagrams are shown in Fig. 4. $\mu_2 = 3.0$ is unchanged. Obviously, for $\mu_1 > \mu_2 = 3.0$, the spiral 1 keeps being the driving spiral, whereas for $\mu_1 < \mu_2 = 3.0$, the fast spiral 2 becomes the driving spiral. The detailed subtypes $1'$ and $4'$ are also illustrated in Figs. 4(c) and 4(d). In addition, all different types of pattern formation and their corresponding FFT's for different system parameters are displayed in Fig. 5, which is quite similar to Fig. 2 again.

To show this unique high-frequency dominance more clearly, in Fig. 6 we plot ω_{1c} (open triangles) and ω_{2c} (open circles) as functions of α with all other parameters fixed: $\beta = -1.0$, $e = 0.5$, $\mu_1 = 14.0$, and $\mu_2 = 3.0$. Obviously for both the outward-rotating spiral for $\alpha < \alpha_c$ (left of the vertical dashed line) and the inward-rotating spiral for $\alpha > \alpha_c$ (right of the vertical dashed line), the patterns of ω_{2c} jumping from two values to one single large value just prior to the phase-synchronization region are the same. Here $\alpha_c \approx 0.075$. Within the phase-synchronization region, ω_{1c} and ω_{2c} become identical.

IV. TWO COUPLED IDENTICAL SPIRALS

Clearly the dynamics of two coupled spirals should be determined by the following four major factors: the system parameters (such as μ, α, and β), the coupling strength e, the relative sense of rotation (the same or opposite chiralities), and their initial separation distance d. So far the first two factors have been well studied in two spirals having the same chirality and a sufficiently large d. For the last two factors, our extensive simulations on different chiralities and d show that, if $\mu_1 \neq \mu_2$, all the above results are robust and unchanged,

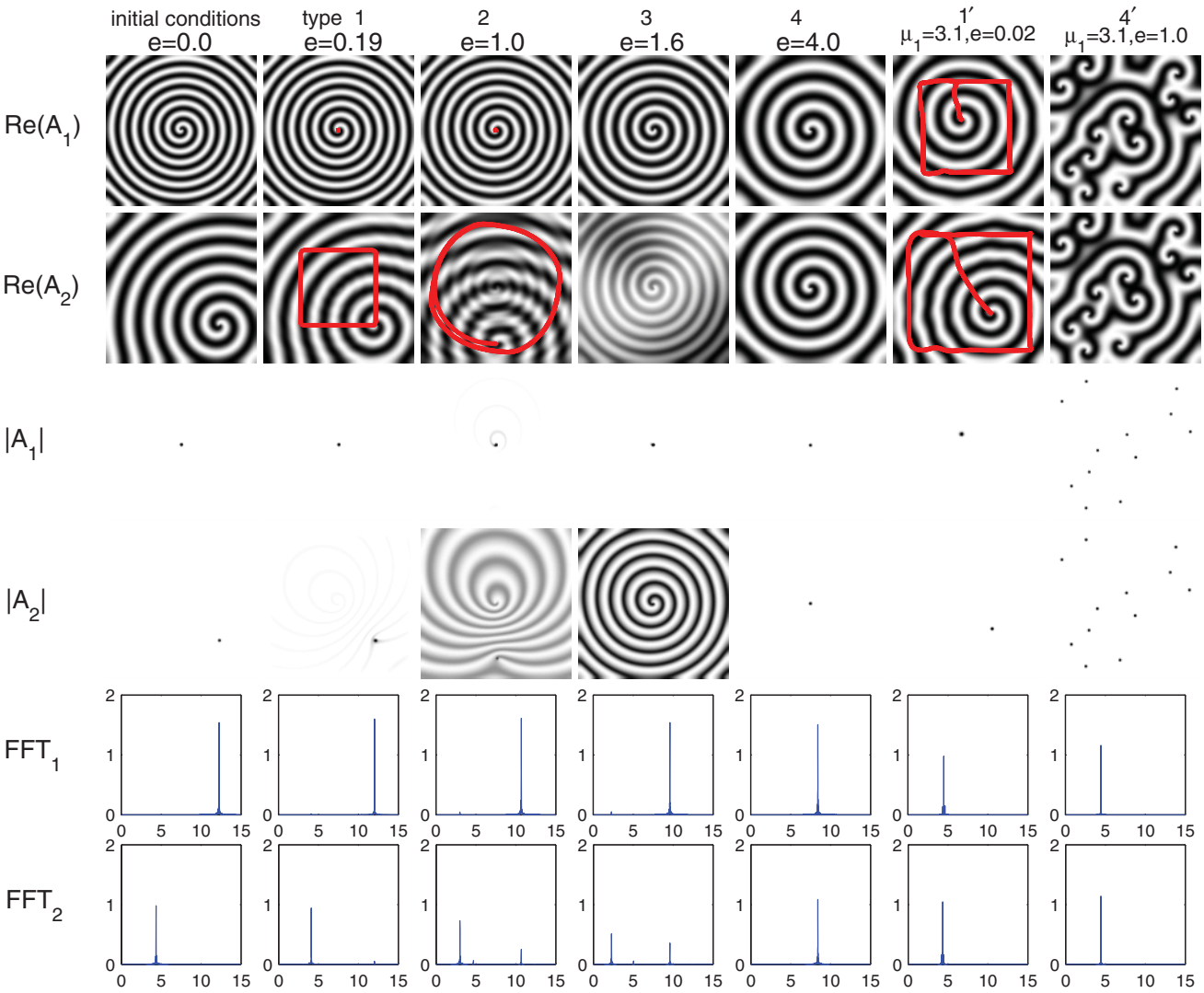

FIG. 5. (Color online) As Fig. 2 but for two coupled inward-rotating spirals. For the first five columns, $\mu_1 = 8.4$.

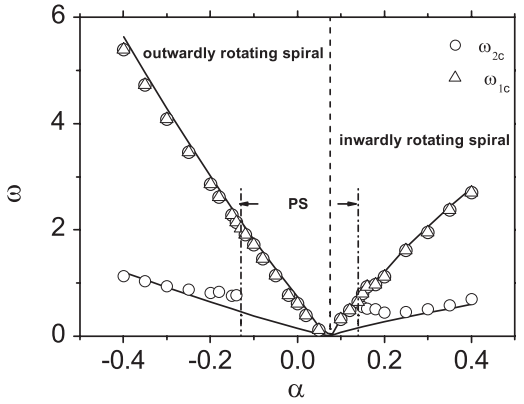

FIG. 6. Plots of ω_{1c} and ω_{2c} vs α, showing the universality of the high-frequency dominance for both the interactions of two outward- and two inward-rotating spirals. The phase-synchronization region is denoted by the letters PS. $\beta = -1.0$, $e = 0.5$, $\mu_1 = 14.0$, and $\mu_2 = 3.0$.

but if $\mu_1 = \mu_2$, these two factors do play a significant role. Therefore, for the nonidentical case, the system parameter effect is dominant. In this section we will focus on the study of two coupled identical spirals ($\mu_1 = \mu_2 = 3.0$). $\alpha = -0.4$ and $\beta = -1.5$ within the outward-rotating spiral parameter region, the same as in Figs. 1–3.

Table I summarizes all the different types of dynamics for $\mu_1 = \mu_2$. Obviously, they change with e, d, and the relative sense of rotation (either corotating or antirotating). Some typical eventual patterns are presented in Fig. 7. For $e < e_c$, if the two spirals are corotating, synchronization appears for a small d ($d < d_c$), but for a large d ($d > d_c$) the spirals drift on an identical circular trajectory but with a different phase, represented as circular drifting in Table I. Here $e_c \approx 0.04$, as shown by the critical point in Figs. 1(c) and 1(d). $d_c \approx 10$. In contrast, for two antirotating spirals, we find that the coupling always leads to a parallel drift of the spiral tips (represented as parallel drifting in Table I), and it is independent of d. These behaviors are intuitively understandable: for a small e, corotating spirals with a small d will always give rise to a complete synchronization (as a stable attractor), whereas for other conditions, only double phase driftings for type $1'$ are possible.

Correspondingly, if $e > e_c$, corotating spirals with a small d will always lead to two completely synchronized spirals showing only one tip (represented as synchronized and single spiral in Table I). However, for other cases, synchronized spirals with multiple spiral tips are generally observed.

Based on these observations, the effects of coupling, initial distance, and relative rotation direction in the interaction of two coupled identical spirals have become clear, and the phase diagram in Fig. 1 is complete.

V. COMPARISON WITH TWO COUPLED SPIRALS IN MONOLAYER MEDIA

Now the differences of the dominant effect between the interaction of two spiral waves in bilayer systems and that in monolayer systems have become clear, and all different types of pattern for the slower forced spiral, including phase drifting, amplitude modulated, and amplitude dominated, have been well recognized in the synchronization scenario. A pure one-way effect has been uncovered under the condition of a mutual two-way coupling. All these classifications and findings provide a useful paradigm for the pattern competition of two spatially extended systems. Compared with the horizontal line-to-line interaction of two wave fronts from the point sources (tips) of two spiral waves in one spatial domain [12], clearly now it is a vertical surface-to-surface interaction. The origin of these generic behaviors must come from this type of global coupling and the spatial extension of the medium as well. Unlike the invasion of the faster spiral into the domain of the slower one, even driving it out of the domain completely, here the dynamics is different, with the pattern in the response system sustained. The other key difference is that now the high-frequency dominant effect is absolute, independent of whether the spirals are outwardly or inwardly rotating. These discoveries are expected to be valuable for an improved understanding of not only the interaction of two spirals in such a quasi-three-dimensional system, but also scroll wave dynamics in truly three-dimensional systems [37]. They might also be helpful for potential applications in the control of spiral waves [38,39].

VI. COMPARISON WITH PREVIOUS WORKS ON TWO COUPLED SPIRALS IN BILAYER MEDIA

In this section, it is worthwhile to give some more comparisons with earlier relevant results. In this paper, we find that, as e increases, the slower spiral may gradually show phase-drifting, amplitude-modulated, amplitude-dominated, and phase-synchronized patterns. Actually, all these various patterns have been reported in the literature. For instance, phase drifting was found in Ref. [23], amplitude modulation was reported in Ref. [18] as a transient behavior, amplitude domination was discovered recently in Ref. [26], and phase synchronization occurs as a common behavior if e is large

TABLE I. Description of two coupled identical spirals ($\mu_1 = \mu_2$) for three important effects: the coupling strength e (either $e < e_c$ or $e > e_c$), initial separation distance d (either $d < d_c$ or $d > d_c$), and relative rotation direction (either corotating for identical chiralities or antirotating for opposite chiralities). $e_c \approx 0.04$, indicated by the black point in Figs. 1(c) and 1(d). See the text for more details.

	$e < e_c$	$e > e_c$	
Small d	Synchronized and single spiral	Synchronized and single spiral	Corotating
	Parallel drifting	Synchronized and multispiral	Antirotating
Large d	Circular drifting	Synchronized and multispiral	Corotating
	Parallel drifting	Synchronized and multispiral	Antirotating

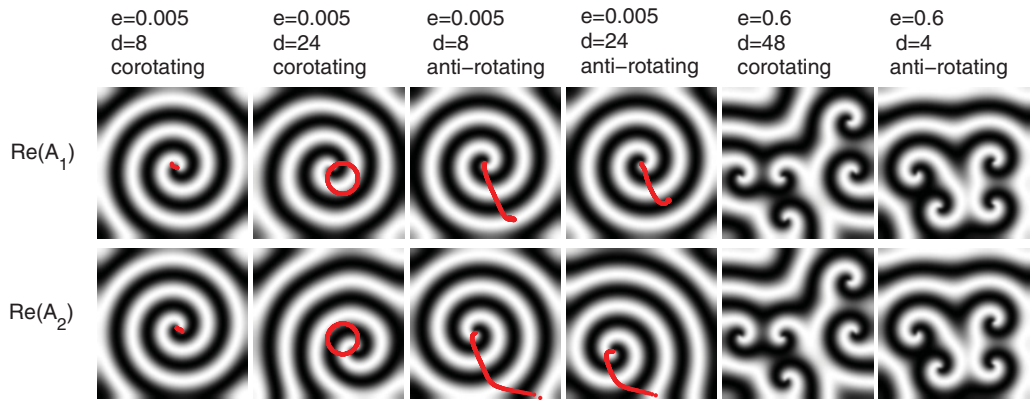

FIG. 7. (Color online) Some typical patterns of two coupled identical spirals, showing the remarkable impacts of initial conditions for different separation distances and relative rotations under the condition of two identical systems ($\mu_1 = \mu_2$).

[18,23,26]. Therefore, it seems that all these behaviors, now found to simply depend on different values of the frequency discrepancy and coupling strength, can be well combined in a single model. As a result, the synchronization scenario can be understood in a comprehensive way.

For the other important effect, the so-called high-frequency dominance, which was reported in Ref. [18] in a chemical experiment and in Ref. [23] in a numerical study, we extend it to the antispiral parameter region and find it is unchanged. In addition, we find that it is independent of the initial conditions. In the simulations of coupled Bär reaction-diffusion systems [23], two different cases including the resonant case for a small frequency mismatch and the nonresonant case for a large one were studied. In particular, for the resonant case, one oscillatory spiral was coupled with another excitable spiral with a small frequency mismatch. Therefore, some findings (e.g., the dependence of high-frequency dominance on initial conditions) reported there may not be relevant to our system.

For two identical spirals, the classification of all the various dynamical behaviors, which depend on the choice of initial conditions, is also remarkable. Some of them have been reported by Hildebrand *et al.* [19], such as the parallel drift for two antirotating spirals and the circular drift for two corotating spirals. However, two phenomena reported there, the spiral breakup and resonance attractors for a discrete set of circular-drifting diameters, have not been observed by us; the reason might come from the fact that in Ref. [19] excitable (not oscillatory) media were treated.

To summarize, we have considered all major factors in the interaction of coupled spirals in bilayer oscillatory media and uncovered a number of interesting results. They provide coherent insight into our improved understanding of spiral wave dynamics.

VII. COMPARISON WITH TWO COUPLED PHASE OSCILLATORS

Finally, it is interesting to further compare with the dynamics of two coupled phase oscillators written as [5]

$$\dot{\theta}_{1,2}(t) = \mu_{1,2}\omega_0 + e\sin(\theta_{2,1} - \theta_{1,2}), \tag{2}$$

where μ_1 and μ_2 are scales for the natural frequencies of the oscillators, ω_0 is the normalized frequency, and e denotes the coupling strength. Without losing generality, $\mu_2 = 3.0$ and $\omega_0 = 1.0$ are chosen.

These two coupled oscillators can transit to phase synchronization showing an identical frequency $\omega_{1c} = \omega_{2c}$, where

$$\omega_{ic} = \lim_{T\to\infty}\frac{1}{T}\int_0^T \dot{\theta}_i(t)dt, \tag{3}$$

as e is larger than a threshold e_c. Considering the phase difference $\Delta\theta = \theta_1 - \theta_2$ to be independent of time after $e \geqslant e_c$ and analyzing its stability, we can easily obtain the critical condition for phase synchronization:

$$e_c = \frac{\omega_0}{2}|\mu_1 - \mu_2|, \tag{4}$$

or equivalently

$$\mu_{1c} = \mu_2 \pm 2e/\omega_0. \tag{5}$$

These two synchronization-desynchronization critical lines in Eq. (5) are plotted in the phase diagram in Fig. 8(a), where

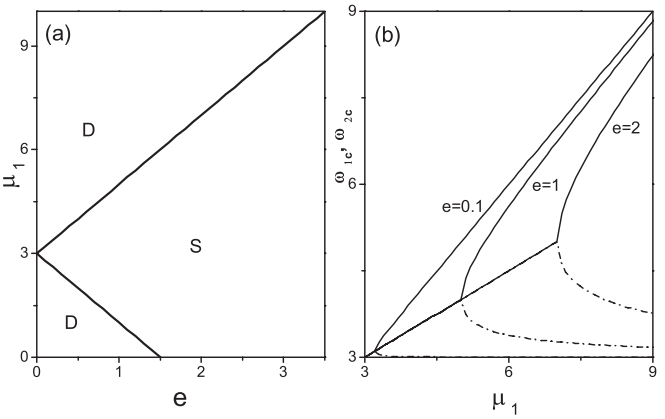

FIG. 8. Study of two coupled phase oscillators (2), showing the absence of dominance effect. (a) Phase diagram for (phase) synchronization and desynchronization behaviors, denoted by the letters S and D, respectively. (b) ω_{1c} (solid lines) and ω_{2c} (dash-dotted lines) vs μ_1 for different e's. Here the actual coupling effect is two way. $\mu_2 = 3.0$ and $\omega_0 = 1.0$.

the two letters D and S indicate the (phase) desynchronization and synchronization regions, respectively. A regular tongue structure is apparent in the (e,μ_1) parameter plane. We also numerically integrated Eq. (2) and calculated ω_{1c} and ω_{2c} for different μ_1's and e's; the results are shown in Fig. 8(b), where solid (dash-dotted) lines are for oscillator 1 (2). As μ_1 decreases, ω_{1c} (ω_{2c}) decreases (increases), and their difference vanishes after $\mu_1 \leqslant \mu_{1c}$, signaling the establishment of phase synchronization. These continuously changing behaviors are fundamentally different from the discrete sharp jumping behaviors seen in Figs. 3(a), 3(c), and 6 for two coupled spiral waves. Here the action between two oscillators is bidirectional, and the so-called asymmetric dominant effect disappears. Therefore, based on these comparisons, we understand that the rich dynamics and high-frequency dominance in coupled spirals reported in the present work are indeed collective behaviors between spatially extended systems, which are unobservable in coupled oscillators in the absence of spatial extension.

ACKNOWLEDGMENTS

This work was partially supported by the Bairen Jihua Foundation of the Chinese Academy of Sciences and the National Natural Science Foundation of China under Grant No. 11075202. We thank the two reviewers very much for their comments and suggestions.

[1] A. T. Winfree, *When Time Breaks Down* (Princeton University Press, Princeton, NJ, 1987).
[2] *Chemical Waves and Patterns*, edited by R. Kapral and K. Showalter (Kluwer, Dordrecht, 1995).
[3] J. Murray, *Mathematical Biology* (Springer, Berlin, 1989).
[4] M. Cross and P. Hohenberg, Rev. Mod. Phys. **65**, 851 (1993).
[5] Y. Kuramoto, *Chemical Oscillations, Waves, and Turbulence* (Springer, New York, 1984).
[6] S. C. Müller, T. Plesser, and B. Hess, Physica D **24**, 87 (1987).
[7] P. Imbihl and G. Ertl, Chem. Rev. (Washington, DC) **95**, 697 (1995).
[8] T. Bohr, G. Huber, and E. Ott, Physica D **106**, 95 (1997).
[9] M. Zhan, J. M. Luo, and J. H. Gao, Phys. Rev. E **75**, 016214 (2007).
[10] J. M. Luo, B. S. Zhang, and M. Zhan, Chaos **19**, 033133 (2009).
[11] K. J. Lee, Phys. Rev. Lett. **79**, 2907 (1997).
[12] V. I. Krinsky and K. I. Agladze, Physica D **8**, 50 (1983).
[13] F. G. Xie, Z. L. Qu, J. N. Weiss, and A. Garfinkel, Phys. Rev. E **63**, 031905 (2001); **59**, 2203 (1999).
[14] M. Hendrey, E. Ott, and T. M. Antonsen, Phys. Rev. Lett. **82**, 859 (1999); Phys. Rev. E **61**, 4943 (2000).
[15] M. Zhan, X. G. Wang, X. F. Gong, and C. H. Lai, Phys. Rev. E **71**, 036212 (2005).
[16] M. Zhan and J. M. Luo, Chaos Solitons Fractals **40**, 229 (2009).
[17] F. G. Xie and J. N. Weiss, Phys. Rev. E **75**, 016107 (2007).
[18] D. Winston, M. Arora, J. Maselko, V. Gáspár, and K. Showalter, Nature (London) **351**, 132 (1991).
[19] M. Hildebrand, J. X. Cui, E. Mihaliuk, J. C. Wang, and K. Showalter, Phys. Rev. E **68**, 026205 (2003).
[20] L. F. Yang, M. Dolnik, A. M. Zhabotinsky, and I. R. Epstein, Phys. Rev. Lett. **88**, 208303 (2002).
[21] I. Berenstein, M. Dolnik, L. F. Yang, A. M. Zhabotinsky, and I. R. Epstein, Phys. Rev. E **70**, 046219 (2004).
[22] I. R. Epstein, I. B. Berenstein, M. Dolnik, V. K. Vanag, L. F. Yang, and A. M. Zhabotinsky, Philos. Trans. R. Soc. London, Ser. A **366**, 397 (2008).
[23] H. J. Yang and J. Z. Yang, Phys. Rev. E **76**, 016206 (2007).
[24] G. Y. Yuan, G. C. Zhang, G. R. Wang, and S. G. Chen, Commun. Theor. Phys. **43**, 459 (2005).
[25] Q. Wang, Q. Y. Gao, H. P. Lü, and Z. G. Zheng, Commun. Theor. Phys. **53**, 977 (2010).
[26] J. H. Gao, L. L. Xie, H. C. Nie, and M. Zhan, Chaos **20**, 043132 (2010).
[27] H. C. Nie, L. L. Xie, J. H. Gao, and M. Zhan, Chaos **21**, 023107 (2011).
[28] L. F. Yang and I. R. Epstein, Phys. Rev. Lett. **90**, 178303 (2003).
[29] L. Junge and U. Parlitz, Phys. Rev. E **62**, 438 (2000).
[30] M. van Hecke, C. Storm, and W. van Saarloos, Physica D **134**, 1 (1999).
[31] S. Boccaletti, J. Bragard, F. T. Arecchi, and H. Mancini, Phys. Rev. Lett. **83**, 536 (1999).
[32] J. Bragard, S. Boccaletti, and H. Mancini, Phys. Rev. Lett. **91**, 064103 (2003).
[33] J. Bragard, S. Boccaletti, C. Mendoza, H. G. E. Hentschel, and H. Mancini, Phys. Rev. E **70**, 036219 (2004).
[34] C. T. Zhou, Chaos **16**, 013124 (2006).
[35] I. S. Aranson and L. Kramer, Rev. Mod. Phys. **74**, 99 (2002).
[36] Y. Gong and D. J. Christini, Phys. Rev. Lett. **90**, 088302 (2003); L. Brusch, E. M. Nicola, and M. Bär, *ibid*. **92**, 089801 (2004); Y. Gong and D. J. Christini, *ibid*. **92**, 089802 (2004).
[37] Z. L. Qu, F. G. Xie, and A. Garfinkel, Phys. Rev. Lett. **83**, 2668 (1999).
[38] D. M. Goldschmidt, V. S. Zykov, and S. C. Müller, Phys. Rev. Lett. **80**, 5220 (1998).
[39] O. U. Kheowan, V. S. Zykov, O. Rangsiman, and S. C. Müller, Phys. Rev. Lett. **86**, 2170 (2001).